The Effect of Nanosilica Concentration on the Enhancement of Epoxy Matrix Resins for Prepreg Composites

Steven C. Hackett, James M. Nelson, Andrew M. Hine, Paul Sedgwick, Robert H. Lowe
3M Composite Materials, Industrial Adhesives and Tapes Division

Douglas P. Goetz, William J. Schultz
3M Corporate Research Materials Laboratory

3M Center
St. Paul, MN 55144

ABSTRACT

Epoxy nanocomposite matrix resins filled with spherical silica particles were investigated at nanosilica loading levels from 0 to 45 % by weight. The effect of silica concentration on neat resin properties was thoroughly evaluated. Important composite matrix resin mechanical properties including modulus and fracture toughness showed significant, monotonically increasing improvement with increasing nanosilica concentration. Desirable changes in coefficient of thermal expansion, cure exotherm, and hardness were also measured. Silica concentration levels did not adversely affect the cured glass transition temperature or prepreg processability. Properties of carbon fiber laminates made with unidirectional prepregs of varying silica loading levels revealed significant improvements in compression strength, in-plane shear modulus, and 0° flexure strain. The properties of the nanocomposite matrix system studied here have led to the commercialization of 3M™ Matrix Resin 3831, in which silica nanoparticle technology enables unique and significant composite property improvements.

1. INTRODUCTION

1.1 Background

The matrix material properties of continuous fiber reinforced composites have a primary effect on both composite compression strength and intra- and interlaminar cracking resistance. Matrix stiffness is a primary variable affecting composite compression strength because fiber microbuckling, a major compression failure mechanism, depends on the amount of support provided by the matrix to the fibers. This has been studied extensively both experimentally and theoretically [1-7]. Fiber waviness, matrix stress-strain curve nonlinearity, and the fiber/matrix interface strength have been identified as important factors [6, 7], but virtually all work on compression mechanisms includes the role of the matrix constitutive behavior. The matrix fracture resistance, along with adequate fiber/matrix interface strength, is important in resisting both interlaminar and intralaminar cracking. The requirements of high matrix stiffness for adequate composite compression strength and high matrix fracture resistance for adequate composite cracking resistance can force compromises since some strategies for increasing fracture resistance of resins reduce modulus [8, 9].

Incorporation of hard particles into polymers increases modulus, and can increase fracture resistance [9]. Micron-scale inorganic fillers have been used to modify cured resin properties, but when processed into fiber-reinforced composite structures, these large particles are filtered out by the reinforcing fibers (Figure 1). Another undesirable effect of conventional fillers is increased resin viscosity before cure, which can compromise composite processing.

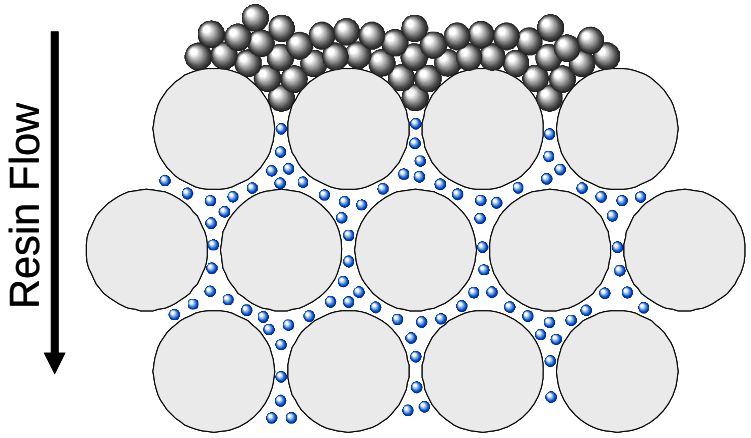

Figure 1. Illustration of filtering of larger particles by fiber array and infiltration of smaller particles between fibers.

1.2 Current Study

In this study, the desirable resin modulus and composite property improvements from inorganic filler modification of a thermosetting matrix resin are achieved through the incorporation of nanoscale particles, in this case, amorphous silica. Nanoscale silica has been shown to simultaneously increase both modulus and fracture resistance, as well as improving other resin properties [10-13]. The highly compatible nature of the functionalized particles enables epoxy resins with levels of nanosilica over 50 wt%. The nanosilica particles form non-aggregated dispersions at all loading levels.

The non-agglomerated compatibilized nanosilica can be evenly dispersed throughout a fiber composite structure without filtration by the fiber array, as illustrated in Figure 1. Figure 2 shows a representative composite laminate not used in this study having 36 wt% nanosilica of nominally 154 nm diameter. The particles have penetrated between 7μm diameter carbon fibers.

Previous studies have also incorporated spherical nanoscale silica into composite matrix resins [e.g., 10, 14-16]. Of particular relevance to this paper is work directed at the increase of composite compression strength [16, 17].

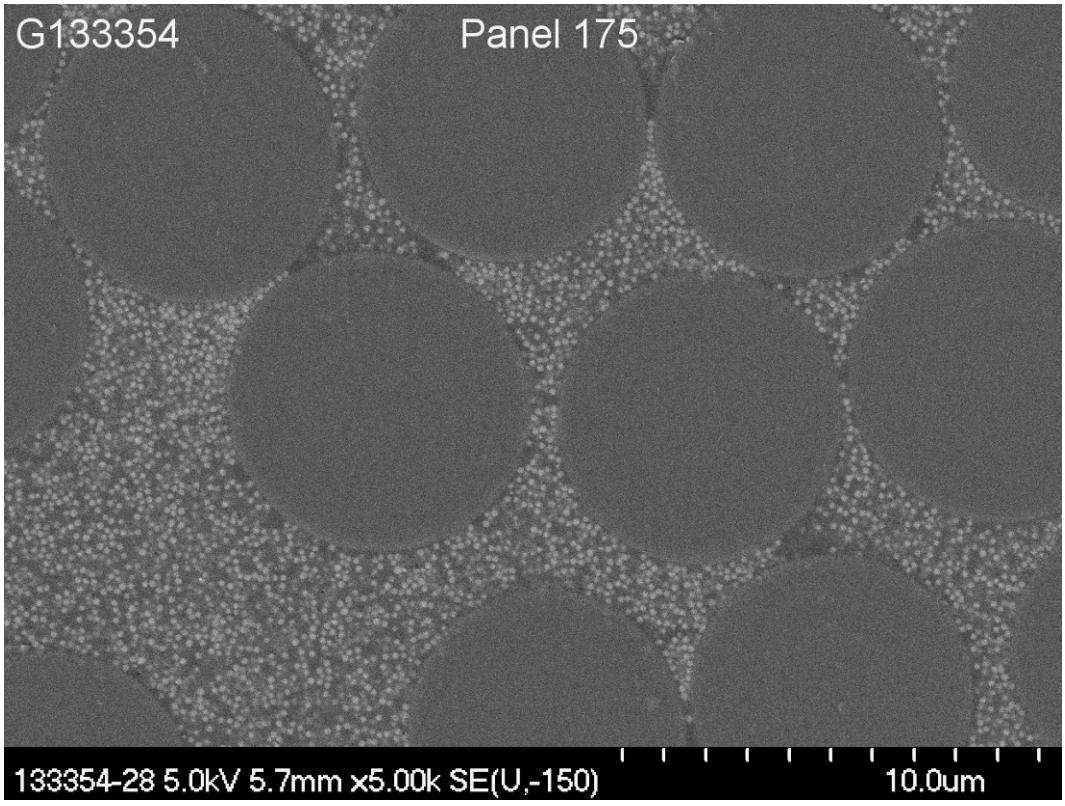

Figure 2. SEM image of a polished 7 micron diameter carbon fiber composite cross-section showing distribution of 154 nm diameter nanosilica

This paper outlines the unique properties of a nanosilica-filled resin technology for prepreg manufacturing processes as a function of silica content. This appears to be the first evaluation of the effects of nanosilica on a prepreg resin system. Emphasis is on very high loading of particles, up to 45% by weight. Unidirectional carbon fiber reinforcement is used at a nominal fiber volume fraction of 60%. This reinforcement scheme is in contrast to previous work using nanoscale silica for composite matrix modification which addressed lower concentrations of particles and either glass fiber reinforcement or low fiber volume fraction carbon fiber reinforcement [14-17]. As a function of nanosilica concentration, this study examines: a) the processibility of the resin for prepreg, b) the quality of nanoparticle dispersion, c) neat resin physical and mechanical properties, and d) carbon fiber laminate mechanical property enhancements. A newly-developed commercial prepreg resin, 3M™ Matrix Resin 3831, which exemplifies the enhanced properties revealed in this study will be highlighted.

2. EXPERIMENTAL

2.1 Materials and Resin Sample Preparation

Resin samples were generated by dilution of an epoxy blend suitable for prepreg manufacturing having 48 wt% silica of nominal particle size 84 nm. Final silica contents of cured resins were 45, 35, 25, and 15 wt%. A control sample containing no silica was also made. A dicy/urea-based cure package was blended into the pre-warmed (80 °C),

nanosilica-filled epoxies with a DAC 600 SpeedMixer (Flacktek, Landrum, SC) at 2350 rpm for 45 seconds to produce well-dispersed blends. These blends were degassed under vacuum for 3-5 minutes prior to being poured into appropriate molds for neat resin tensile testing, dynamic mechanical analysis (DMA), and determination of hardness, coefficient of thermal expansion (CTE), density, moisture absorption, and fracture toughness. The samples were cured in a forced air oven for 2 hours at 90 °C and then for an additional 2 hours at 150 °C.

2.2 Uncured Resin Test Methods

Rheological analyses of these nanosilica-epoxy resin/curative systems were conducted on an ARES rheometer (TA Instruments, New Castle, Delaware) in parallel plate dynamic mode. Samples 25 mm in diameter (25 mm diameter top plate, 40 mm diameter bottom plate) and 1 mm thick were heated from 30 °C to 130 °C at a ramp rate of 2 °C/min, at a frequency of 1 Hz and a strain of 2%.

The cure exotherm was obtained using a modification of ASTM D 3418-08. Uncured resin samples were heated from -30 °C to 300 °C at 10 °C/min.

Linear shrinkage of the resins during cure was measured using ASTM D 2566-86. All interior surfaces of a semi-cylindrical steel trough mold of dimensions 2.54 cm diameter by 25.4 cm length were coated with mold release. The mold was preheated to 90 °C and the liquid resin was poured into the mold. After 2 hrs, the temperature was increased to 150 °C and held for an additional 2 hours. Upon cooling to room temperature, the sample length and the mold length were measured and linear shrinkage was calculated.

2.3 Cured Resin Test Methods

Resin silica content was determined using a 5 to 10 mg cured sample placed in a TA Instruments TGA 500 thermogravimetric analyzer (TA Instruments, New Castle, Delaware). Samples were heated in air from 30 °C to 850 °C at 20 °C/min. The noncombustible residue was taken to be the resin's original nanosilica content.

Flexural storage modulus, E', and glass transition temperature, T_g, of cured resins was obtained by Dynamic Mechanical Analysis (DMA) using an RSA2 Solids Analyzer (Rheometrics Scientific, Inc, Piscataway, NJ) in the dual cantilever beam mode. Experiments were performed using a temperature ramp of -30 °C to 220 °C at 5 °C/minute, a frequency of 1 Hz, and a strain of 0.03 to 0.10%. The peak of the tan delta curve was reported as the T_g.

Density of cured resin specimens was measured by ASTM D 792-86, Test Method B where n-heptane (d = 0.684 g/cc) was used as the immersion liquid. For each material, four specimens were measured and the average specific gravity was reported in g/cc.

Barcol hardness (H_B) was measured according to ASTM D 2583-95 (Reapproved 2001). A Barcol Impressor (Model GYZJ-934-1, available from Barber-Colman Company, Leesburg, VA) was used to make measurements. For each specimen, between 5 and 10 measurements were made and the average value was reported.

Coefficient of thermal expansion (CTE) measurements were performed using a TMA Q400 (TA Instruments) with a macroexpansion probe. A force of 1.0 N was applied and

the specimen lengths were measured at room temperature. The specimens were cooled to -25 °C, heated to 175 °C, cooled back down to -25 °C, then heated a second time to 175 °C. The CTE was taken to be a curve fit from 0 °C to 50 °C on the second heat.

Moisture absorption determinations were conducted using cured resin plaques with dimensions of 20 mm by 20 mm by 2 mm. Specimens were dried for 16 hours at 100 °C in a desiccator. After initial weighing, the specimens were placed in a Thermotron SE-1000-3 (Thermotron Industries, Holland, MI) environmental chamber set at 85 °C and 85% relative humidity. Samples were weighed at 24 hour intervals for the first 14 days and at regular intervals thereafter for over 8 weeks.

Fracture toughness was measured according to ASTM D 5045-99 using a compact tension geometry, wherein the specimens had nominal dimensions of 3.18 cm by 3.05 cm by 0.64 cm with W = 2.54 cm, a = 1.27 cm, and B = 0.64 cm. A modified loading rate of 1.3 mm/minute (0.050 inches/minute) was used.

The tensile strengths, failure strains, and moduli of the resins at room temperature were measured according to ASTM D638 using a "Type I" specimen. The loading rate was 1.3 mm/min (0.05 in/min). Five specimens were tested for each concentration level.

The fracture surfaces generated by fracture toughness testing were imaged using a Philips XL30 ESEM TMP scanning electron microscope (SEM) in high vacuum mode. The surfaces were sputtered with an Au-Pd coating.

A Hitachi H-9000 transmission electron microscope (TEM) was used to examine prepared samples. Cured samples for TEM observation were microtomed at room temperature. All samples were cut at the thickness of 87 nm so that a direct comparison could be made between the different wt% particle loadings.

2.4 Carbon Fiber Composite Sample Preparation

Unidirectional prepreg tape for each of the resin systems was produced by Patz Materials and Technologies (Benicia, CA) using TR50S carbon fiber (Grafil Inc., Sacramento, CA). The 30.48 cm wide unidirectional prepregs had nominal fiber areal weights of 145 g/m^2.

Composite laminates were prepared using typical vacuum bag techniques to achieve porosity-free samples. Laminates were heated from room temperature to 127 °C at 6.7 °C/min using 5.9 bar of pressure. The laminates were cured at 127 °C for 2 hours, then were allowed to slowly cool to below 37 °C before removal.

Three types of laminates were made from each prepreg: a) $[0°]_{12}$ for compression, b) $[0°]_{24}$ for 0° flexure, and c) $[(\pm 45)_4/+45]_s$ for in-plane shear. Nominal cured ply thicknesses were 0.129 mm. A wet diamond saw was used to cut specimens.

2.5 Carbon Fiber Composite Test Methods

Compression strength of the composite laminates was measured according to the Suppliers of Advanced Composite Materials Association recommended method SRM 1R-94 "Recommended Test Method for Compressive Properties of Oriented Fiber-Resin Composites." Tabs were cut from twelve-ply laminates of a common commercial carbon fiber prepreg tape made using a $[0°,90°]_{3s}$ lay-up. The tabs were bonded using a scrimmed epoxy film adhesive AF163-2 (3M, Saint Paul, MN) so that a consistent gage

section of 4.75 mm was obtained. A "Modified ASTM D695" (Wyoming Test Fixtures, Inc., Salt Lake City, UT) test fixture was used with bolt torques of 113 N-cm. A spherically-seated lower platen and a fixed upper platen were used to compress the specimens at a rate of 1.27 mm/min. Nine specimens of each laminate were tested.

In-plane shear modulus was determined by the procedure of ASTM D 3518 except that a $[(\pm 45)_4/+45]_s$ laminate was used. Eight specimens were tested from each panel. A biaxial extensometer was employed. Following the standard, the shear modulus was taken to be the chord modulus between 2,000 and 6,000 micro-shear-strain.

Flexure testing was conducted following ASTM D790 using a nominal strain rate of (0.10 mm/mm/min). Five specimens measuring 127 x 12.7 x 3.2 mm were cut in the 0° direction from a $[0°]_{24}$ laminate. A span:depth ratio of 32:1was used.

All testing was conducted under ambient laboratory conditions.

3. RESULTS AND DISCUSSION

Tables 1-3 summarize neat resin data for this concentration study.

Table 1. Resin Processing Data

Silica (wt%)	Complex Viscosity @ 71°C (Pa-s)	Minimum Complex Viscosity (Pa-s)	Cure Exotherm (J/g)	Cure Exotherm, T_{max} (°C)	Cure Shrinkage (%)
0	5.8	0.37	471	149.5	0.62
15	9.6	0.52	397	149.7	0.58
25	13.0	0.64	347	150.4	0.54
35	23.0	1.10	319	151.7	0.47
45	48.3	3.68	258	151.6	0.33

Table 2. Resin Mechanical Property Data

Silica (wt%)	E' (GPa)	T_g (°C)	Tensile Properties			Fracture toughness (MPa-$m^{1/2}$)
			Modulus (GPa)	Strength (MPa)	Strain (%)	
0	4.1	183	3.496	65.6	2.35	0.61
15	4.7	181	4.316	57.1	1.55	0.67
25	5.7	181	4.888	65.0	1.62	0.83
35	6.1	181	5.916	63.6	1.31	0.89
45	8.1	181	7.150	71.9	1.19	0.93

Table 3. General Cured Resin Data

Silica (wt%)	Barcol Hardness (H_B)	CTE (µm/m/°C)	Moisture uptake (wt%)	Density (g/cc)	Silica Volume (%)
0	42	48.0	4.9	1.246	0
15	56	41.4	4.3	1.328	9.4
25	63	39.1	4.1	1.393	16.1
35	68	37.1	3.7	1.468	23.4
45	73	31.7	3.3	1.543	31.9

3.1 Effect of Silica Concentration on Processability and Part Fabrication

Resin viscosity during curing is an important criterion for prepreg resin systems. Rheometric analysis using viscosity vs. temperature profiles reveals any possible changes in resin cure profile as a result of increasing silica content. The prepreg manufacturing process requires a resin system with viscosity capable of film formation at a temperature well below the cure temperature. The resin must also flow during cure sufficiently to allow air to be removed from the laminate and to fully wet out all of the fibers. In Table 1 is shown the viscosity of each of the resins at the film-forming temperature of 71 °C. While the viscosity ranged from 5.8 Pa-s for the control to 48.3 Pa-s for the 45 wt% silica sample, all made excellent films and prepregs with suitable tack and drape. The minimum viscosities during cure ranged from 0.37 Pa-s for the unfilled control to 3.68 Pa-s for the 45 wt% sample and excellent low void laminates were made from all of the formulations. Representative viscosity profiles for the resin/curative blends are shown in Figure 3.

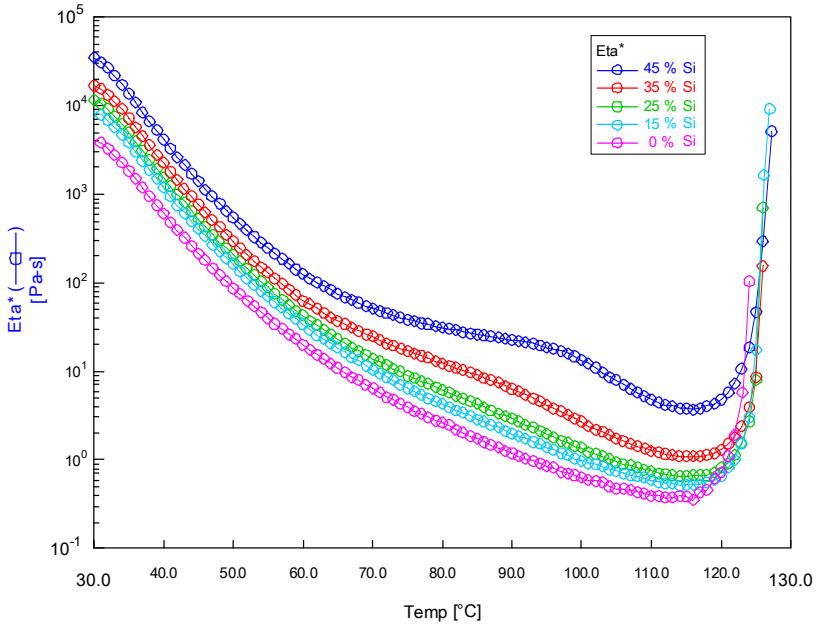

Figure 3. Representative viscosity vs. temperature profiles

An important finding of this work is the reduction of cure exotherm with increasing silica content. The cure exotherm as a function of silica content is shown in Table 1. A 45 % reduction of cure exotherm is measured by the addition of 45 wt% nanosilica. Nanosilica lowers the extent of exotherm during cure by simply reducing the amount of curable resin present. This may be very important for the fabrication of thick parts where heat management during cure is crucial. Also shown in Table 1 are the shrinkage values which show the trend of reduced shrinkage with increased silica content. Both of these features are desirable for composite fabrication.

To probe the effect of silica content on nanoparticle dispersion, TEM micrographs were obtained as a function of silica wt% as displayed in Figure 4. Figure 5 demonstrates that a non-agglomerated, non-aggregated dispersion was produced over the range of 15-45 wt% silica.

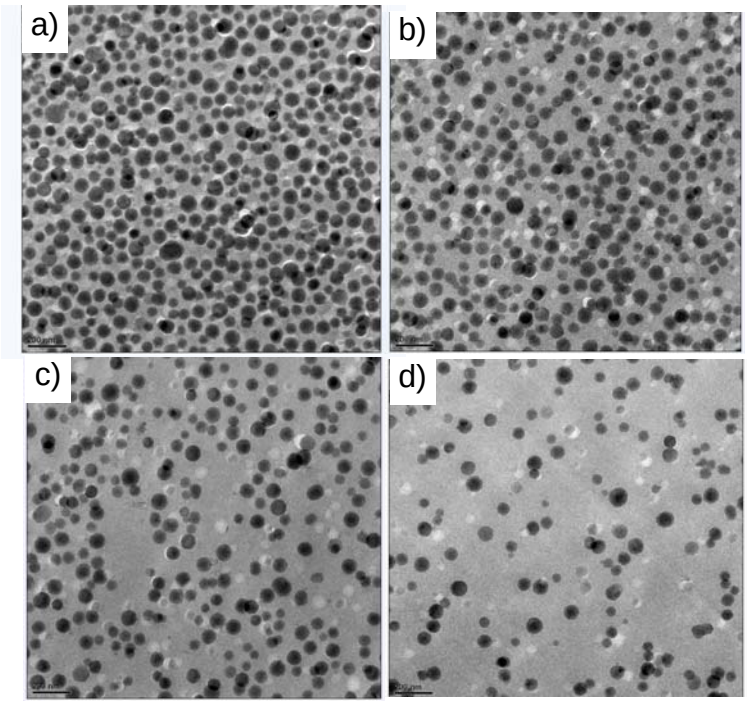

Figure 4. TEM Micrographs of nanosilica dispersion at various nanosilica levels. a) 45 wt%; b) 35 wt%; c) 25 wt%; d) 15 wt% (All at 10,000X instrument magnification)

Reduced coefficient of thermal expansion is desirable for composite matrix materials in order to reduce thermal stresses and part distortion. Silica concentrations of 15-45 wt% resulted in a reduction in the coefficient of thermal expansion as shown in Table 3. For example, incorporation of 45 wt% silica lowered the CTE by 50%. Additionally, increasing silica incorporation leads to an increase in surface Barcol hardness (Table 3). The high hardness enhances durability and part surface quality. Higher hardness, lower CTE, and lower cure exotherm are particularly important in composite tooling applications.

3.2 Effect of Silica Concentration on Cured Resin Properties.

Density was measured on cured resin samples ranging from 0-45 wt% nanosilica and results are displayed in Table 3. The inclusion of nanosilica into a resin increases the density of the resultant system because the density of silica is higher than that of the base resin. The measured densities and weight fractions of silica can be used to verify the nominal density of these particles is 2.2 g/cc, in contrast to the lower density of nanosilica reported elsewhere [12, 13]. Typical carbon fiber prepregs have fiber volume fraction of about 60%, so the increase in density of prepreg-based composites with nanosilica modification is a few percent. As will be seen, the accompanying gain in composite properties offer composite designers latitude in eliminating carbon fiber and other weight- and cost-saving strategies. These can result in an overall reduction in part weight for equal strength or stiffness. Also listed in Table 3 are the corresponding volume % of silica calculated using the measured densities.

Another property affected by the inclusion of nanosilica is moisture uptake during hot/wet conditioning. As displayed in Figure 5, the % weight gain increases as a function of decreasing silica concentration/increasing resin content. The control epoxy sample displays the largest increase in weight. The moisture weight gained agrees closely with a volume percent of the cured base epoxy material. This implies that the contribution to total weight gain by water at the surface of these nanosilica particles is small.

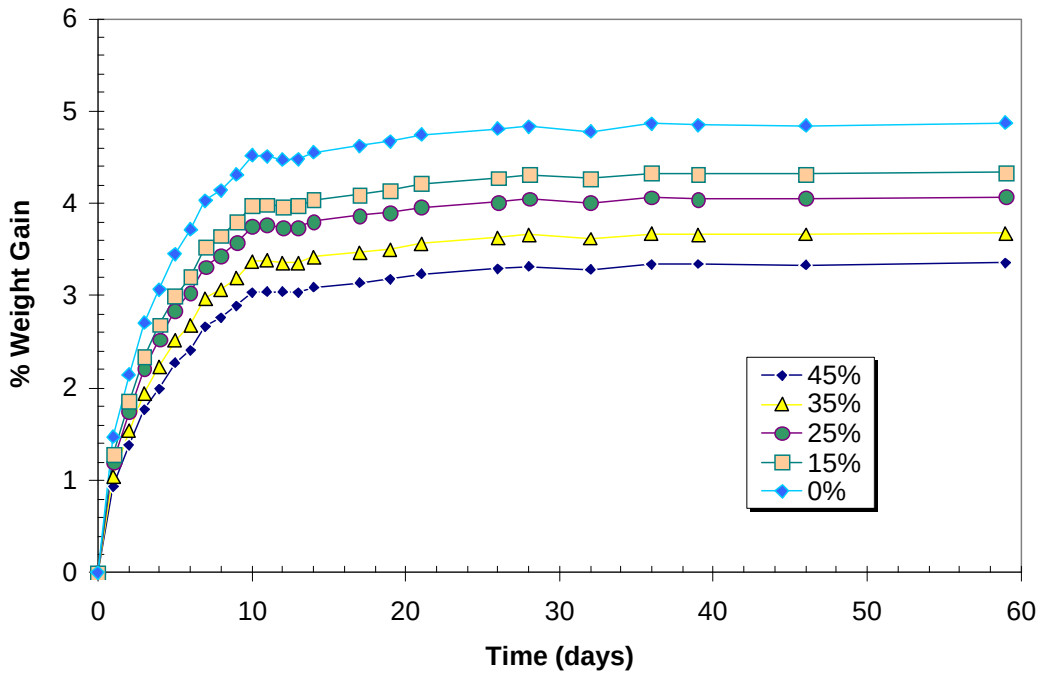

Figure 5. Effect of nanosilica concentration on weight gain during hot/wet conditioning.

Dynamic mechanical analysis of cured samples with varying silica content was undertaken to explore the effect of increasing silica content on resin modulus. Figure 6 shows the storage modulus, E', vs. temperature plotted on a linear scale. As anticipated,

the modulus increased monotonically with increasing silica content throughout the range explored in this study.

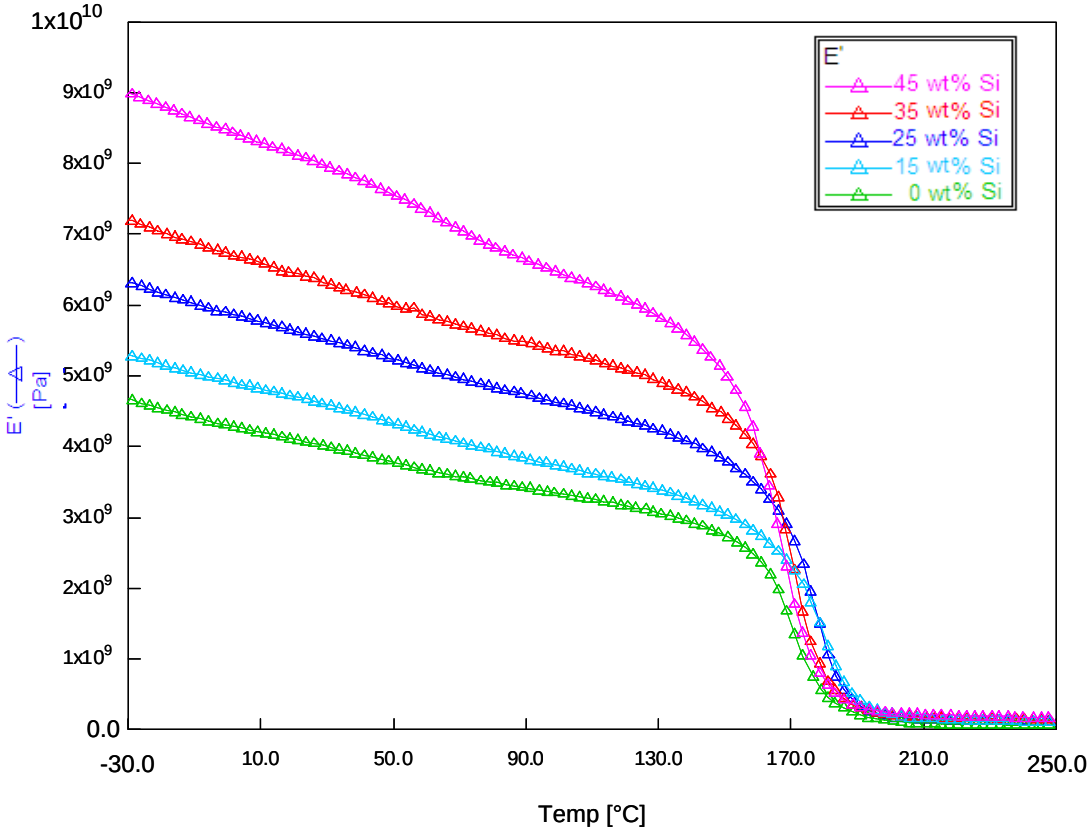

Figure 6. Dynamic mechanical spectra of cured resins

Glass transition temperatures defined by tan delta peaks were determined as a function of increasing silica content and their values are shown in Table 2. T_g values ranged narrowly from 183 to 181 °C, equivalent within the resolution of the measurement technique.

Cured resin tensile tests were performed to directly measure the resin tensile modulus. Table 2 lists the tensile modulus as well as the average stress and strain at failure. At the 45 wt% level of nanosilica, the tensile modulus is double that of the control resin. The variability of failure stress and strain can be attributed to the flaw-sensitive nature of the test. The resin castings contained some undissolved curative. In general, increased silica content appeared to produce similar strength levels with reduced failure strains for this base resin system as the modulus increased.

Results of resin fracture testing are given in Table 2. The critical plane-strain stress intensity factor, K_{IC}, increased monotonically with increasing nanosilica content. The incorporation of 45 wt% silica increased K_{IC} by about 50%. Figure 7 shows the fracture surfaces near the precrack for the unfilled control resin and the 45 wt% silica material at low and high magnifications. The direction of crack propagation in the images is from left to right. In the lower magnification images, undissolved solid curative can be seen. The control has a very smooth surface as examined at both low and high magnifications,

with fine ridges typical of unmodified epoxy. The low magnification image of the fracture surface of the 45 wt% silica resin (Figure 7b) shows whitening at the edge of the precrack due to a change in texture. Significantly coarser ridges emanate from the precrack, and "tails" are seen at the undissolved curative particles. The high magnification Figure 7c shows the nearly featureless surface of the unfilled control, apart from a fine tear ridge. In contrast, the filled material shown in Figure 7d reveals a surface that is rough on the submicron scale. Individual silica particles can be seen, with no aggregation. The magnification used here is insufficient to establish the extent of particle/polymer debonding present, a fracture mechanism discussed by previous investigators of nanoparticle toughening [12, 13, 15].

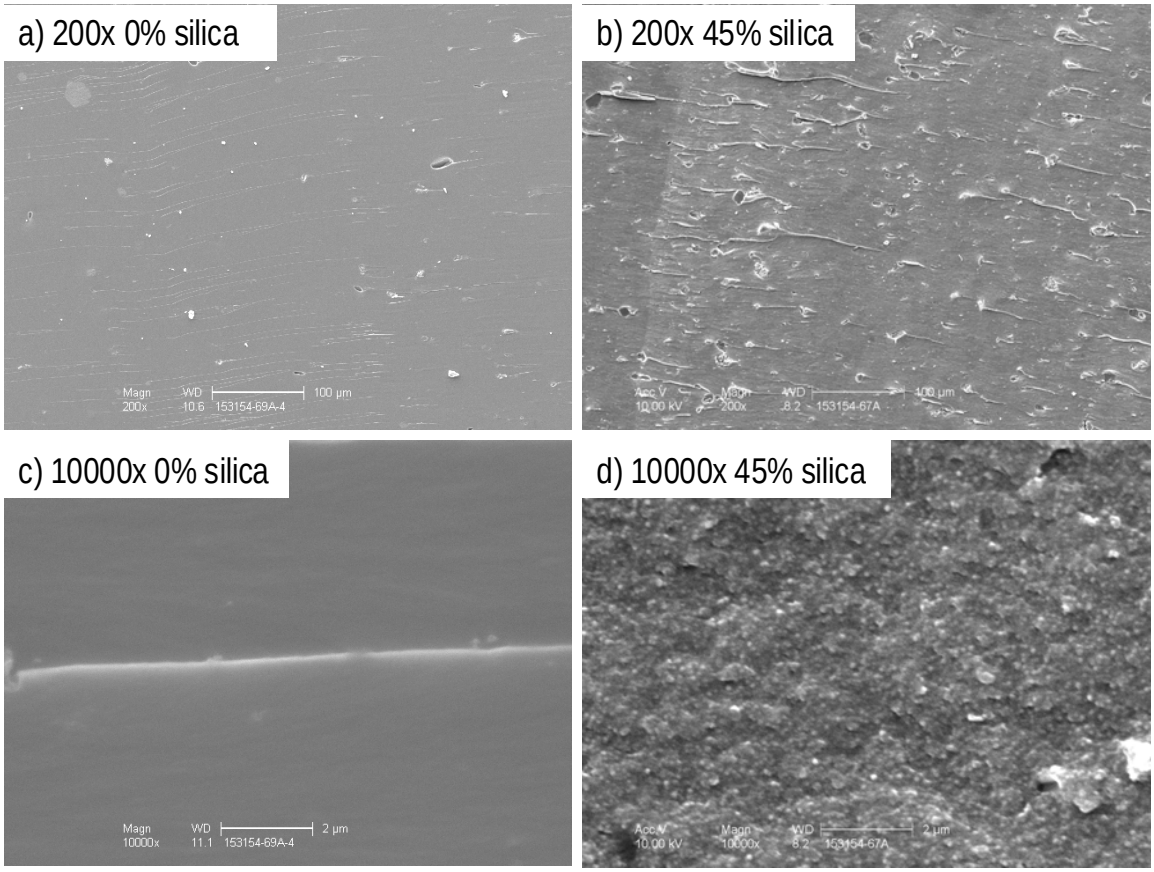

Figure 7. Fracture surfaces of unfilled control and resin with 45 wt% nanosilica. Crack propagation was from left to right.

As discussed in the introduction, both increased matrix modulus and fracture resistance are desirable for fiber reinforced composites. Figure 8 plots the increase in both properties over the entire range of silica concentration examined in this study.

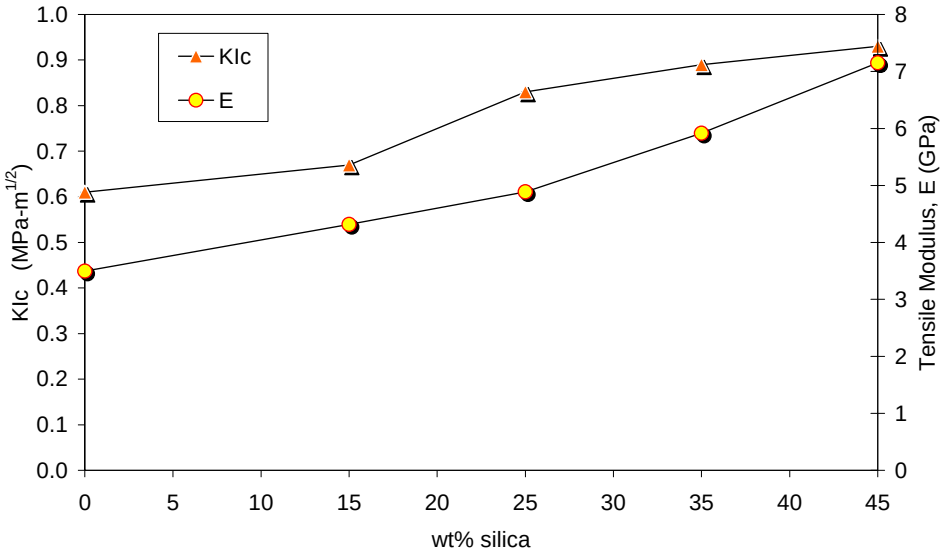

Figure 8. Increasing resin fracture resistance and tensile modulus with increasing nanosilica content

3.3 Effect of Silica Concentration on Composite Mechanical Properties

Table 4. Summary of Nanosilica Epoxy Carbon-fiber Composite Properties

Silica (wt%)	In-plane Shear		SRM-1R94 Compression		0° Flexure		
	Modulus (GPa)	FV (%)	Strength (GPa)	FV (%)	Modulus (GPa)	Strength (GPa)	Strain (%)
0	4.74	62.9	1.779	62.5	126.9	1.53	1.21
15	5.18	61.5	1.841	61.2	128.2	1.68	1.32
25	5.44	60.6	1.889	60.3	126.0	1.71	1.37
35	5.96	61.1	1.903	60.3	126.9	1.83	1.49
45	6.63	60.0	1.979	59.2	124.7	1.93	1.56

As shown in Table 4, in-plane shear modulus increased monotonically with increased nanosilica content. At 45 wt% nanosilica, the increase over the unfilled control was 40%. The tensile modulus of the neat matrix resin reported in Table 2 increased about 100% for this loading. The matrix shear modulus trend is expected to follow that of the matrix tensile modulus closely. Micromechanical considerations preclude one-to-one translation of matrix stiffness to composite shear stiffness due to the presence of fibers. In addition, a difference in definitions should be considered when interpreting the translation of matrix to composite modulus increase. The matrix tensile modulus is determined by the initial slope of the stress-strain curve, while the composite in-plane shear modulus is defined in ASTM D 3518 as the chord modulus between 2000 and 6000 shear

microstrain. For this shear strain range, the composite shear stress-strain curves are nonlinear, so the chord shear modulus is significantly lower than the initial slope of the shear stress-strain curve.

Unidirectional compression strength as measured by SACMA SRM-1R is listed in Table 4. The average strength increased monotonically with increasing nanosilica content. The apparent strength changed by 11.2% at 45 wt% silica loading. This increase is less than expected, given the large change in matrix stiffness. However, note from the table that the fiber volume fraction of the laminates in this series was higher for the prepregs with lower amounts of nanosilica. If the strength values are normalized to 60% fiber volume, the change from the unfilled to the most highly filled material is 17.4%. So variations in fiber volume fraction are likely to have had a significant effect on the measured compression strengths. An additional consideration is the sensitivity of this compression test method to changes in matrix modulus. Previous work [5] using the SRM-1R method explored the effect of varying the matrix modulus by testing at elevated temperatures. In that study the compression strength for unidirectional laminates was found to correspond more strongly to the matrix modulus. The elevated temperature stress-strain curves not only varied in initial modulus, but also nonlinearity. Numerous studies have connected compression strength to nonlinearity of the matrix stress-strain curve [e.g., 4, 6, 7]. It is likely that the sensitivity of the test to matrix variations depends on changes not only to the small-strain modulus, but the entire stress-strain curve. In addition, fiber waviness and interfacial strength have been identified as important variables affecting compression strength. Therefore, the strength of the correlation with matrix modulus may vary depending on other factors. Uddin and Sun [16] found an increase of measured compression strength of up to 41% for 5° off-axis glass fiber composite laminates when the matrix was modified with nanosilica to increase the modulus by 40%. In contrast, Tsai et. al found a much smaller increase even at a higher silica level [17]. These results demonstrate that the overall material system and measurement method are important.

The unidirectional flexure results listed in Table 4 shed additional light on the compression behavior. As expected, the flexural modulus is essentially unchanged with increased silica content, because it is dominated by the fibers and the 32:1 span to depth ratio minimizes the effect of interlaminar shear deformations on deflection. However, flexure strength and strain increase monotonically. Examination of the flex specimens after failure reveals that the failures were compression-dominated. The increase in strength and strain are consistent with the expected dependence on matrix stiffness. The increases were more pronounced than for the compression tests. At the 45% loading level, the flexure strength increased by 26%, and the flex strain at failure increased by 29% over the control.

3.4 Commercial Application of Nanosilica Technology in 3M™ Matrix Resin 3831

In 2009, 3M introduced 3M™ Matrix Resin 3831, a 36 wt% silica content nanocomposite epoxy resin system designed for use in composite prepreg manufacturing processes. This commercial system displays the performance characteristics elucidated in the present study. Initial implementation of this epoxy nanocomposite resin in the sporting goods market has made producing stronger, lighter-weight carbon fiber composites structures such as fishing rods and marine spars possible. Real world

application-based testing of carbon fiber reinforced composite designs containing 3M™ Matrix Resin 3831 have shown dramatic increases in strength such as a 30-50% strength increase in marine spars and a 60-90% strength increase in fishing rods where compression-dominated bending failures occur. This increase in composite compressive properties offers composite engineers greater design flexibility in optimizing the strength, weight, and performance of carbon fiber prepreg structures.

4. SUMMARY

The effect of nanosilica concentration on matrix resin properties was studied. Epoxy nanocomposite resins with high weight fractions of nanosilica offer dramatic enhancements in both resin modulus and fracture toughness. In addition, other resin properties desirable for fiber-reinforced composites were improved. The incorporation of nanosilica loading levels up to 45 wt% produced prepreg resins with suitable characteristics for the prepreg manufacturing process. Carbon fiber prepreg composites incorporating these matrix materials display monotonically increasing shear stiffness, compression strength, and flexural strength with increasing nanosilica concentration.

5. FUTURE WORK

The effect of nanosilica concentration on other composite properties is being explored, and is reported elsewhere [18]. The nanocomposite matrix technology described here is being extended into additional resin systems for prepreg and liquid processing such as resin transfer molding and filament winding that take advantage of the unique attributes of highly-filled matrix materials.

6. ACKNOWLEDGEMENTS

We would like to thank Mary Buckett of 3M's Corporate Research Analytical Laboratory for her assistance with the TEM images, Rachel Wilkerson for neat resin fracture testing, and Dan Quinn for resin sample preparation.

7. REFERENCES

1. Rosen, B.W., "Mechanics of composite strengthening." Fiber Composite Materials, American Society for Metals Seminar (1965): 37-75.

2. Shuart, M.J., "Short-wavelength buckling and shear failures for compression-loaded composite laminates." NASA TM-87640, NASA Langley Research Center, Hampton, VA, Nov. 1985.

3. Camponeschi, E.T. Jr., "Compression of composite materials: a review." *Composite Materials: Fatigue and Fracture (Third Volume) ASTM STP1110.* T.D. O'Brien, Ed., Philadelphia, PA: ASTM (1991): 550-578.

4. Sun, C.T., Jun, A.W., "Compressive strength of unidirectional fiber composites with matrix non-linearity." *Composite Science and Technology.* 52 (1994): 577-587.

5. Goetz, D.P., Hine, A.M., Portelli, G.B. “The dependence of composite lamina compression strength on matrix modulus. ” *Proc Sixth Japan-U.S. Conference on Composite Materials* Orlando, FL, June 22-24, 1992.

6. Guynn, E.G., Bradley, W.L., Ozden, O.O. “A Parametric Study of Variables That Affect Fiber Microbuckling Initiation in Composite Laminates: Part 1-Analyses.” *Journal of Composite Materials* 26 (1992): 1594-1616.

7. Guynn, E.G., Bradley, W.L., Ozden, O.O. “A Parametric Study of Variables That Affect Fiber Microbuckling Initiation in Composite Laminates: Part 2-Experiments.” *Journal of Composite Materials* 26 (1992): 1617-1643.

8. Yee, A.F., Pearson, R.A. “Toughening mechanisms in elasomer-modified epoxies.” *Journal of Materials Science*, 21, (1986): 2462-2474.

9. Kinloch, A.J., Young, R.J. *Fracture Behaviour of Polymers*, London, England: Elsevier Applied Science Publishers Ltd., 1983.

10. US Patent 5,648,407. “Curable resin sols and fber-reinfoced composites derived therefrom.” (1997).

11. Hackett, S., Gross, K., Schultz, W., Thompson, W. “Advanced capillary underfill for flip chip attachment.” *Proc. Surface Mount Technology Association*. Chicago, IL, Sept. 22-26, 2002.

12. Liang, Y.L., Pearson, R.A. “Toughening mechanisms in epoxy-silica nanocomposites (ESNs).” *Polymer* 50 (2009): 4895-4905.

13. Johnsen, B.B., Kinloch, A.J., Mohammed, R.D., Taylor, A.C. Sprenger, S. “Toughening mechanisms of nanoparticle-modified epoxy polymers.” *Polymer*, 48, (2007): 30-41.

14. Kinloch, A.J., Mohammed, R.D., Taylor, A.C., Sprenger, S. Egan, D. “The interlaminar toughness of carbon-fibre reinforced plastic composites using hybrid-toughened matrices.” *Journal of Material Science* 41 (2006): 5043-5046.

15. Hsieh T.H., Kinloch, A.J., Masania, K., Lee, J.S., Taylor, A.C., Sprenger, S. “The toughness of epoxy polymers and fibre composites modified with rubber microparticles and silica nanoparticles.” *Journal of Material Science* 45 (2010): 1193-1210.

16. Uddin, M.F., Sun, C.T. “Strength of unidirectional glass/epoxy composite with silica nanoparticle-enhanced matrix.” *Composites Science and Technology* 68 (2008):1637-1643.

17. Tsai, J-L., Hsiao, H., Cheng, Y-L. “Investigating mechanical behaviors of silica nanoparticle reinforced composites” *Journal of Composite Materials* 44 (2010): 505-524.

18. Hackett, S.C., Nelson, J.M., Hine, A.M., Sedgwick, P., Lowe, R.H., Goetz, D.P., Schultz, W.J. “Improved carbon fiber composite compression strength and shear stiffness through matrix modification with nanosilica” *Proc. American Society for Composites 25th Annual Technical Conference*. Dayton, OH, Sept. 20-22, 2010.